J|A|C|S COMMUNICATIONS

Published on Web 03/18/2010

Structurally Ordered FePt Nanoparticles and Their Enhanced Catalysis for Oxygen Reduction Reaction

Jaemin Kim,[†] Youngmin Lee, and Shouheng Sun*

Department of Chemistry, Brown University, Providence, Rhode Island 02912

Received February 3, 2010; E-mail: ssun@brown.edu

In searching for active catalysts for oxygen reduction reaction (ORR) in the polymer electrolyte membrane fuel cells (PEMFCs), Pt alloyed with early transition metals of Fe, Co, or Ni has attracted great interest.[1] Recent studies on single crystalline thin films have revealed that the addition of an early transition metal to Pt can change the geometric (Pt−Pt bond distance and coordination number) and electronic structures of Pt.[2] Due to these structural changes, the adsorption of OH is mostly centered on the second metal, not on Pt, and oxygen tends to be reduced on Pt in a "four-electron" process. The ORR catalytic activity of these alloys is also dependent on the type and concentration of the second metal in the subsurface atomic layers.[1,3] These early studies on the model alloy catalysts indicate that an alloy nanoparticle (NP) of MPt (M = Fe, Co, or Ni) with an intermetallic structure should serve as a more practical catalyst for ORR.

Here we report on the structure-dependent FePt NP catalysis and demonstrate that the intermetallic FePt NPs are a much better catalyst for ORR. Monodisperse FePt NPs with control on Fe, Pt composition have been synthesized.[4] These FePt NPs have the chemically disordered face centered cubic (fcc) structure within which Fe and Pt atoms are positioned randomly in the fcc lattice (Figure 1A).[5] Under high temperature annealing conditions, the fcc structure can be converted to a chemically ordered face centered tetragonal (fct) structure with Fe and Pt intermetallically stacked (Figure 1B). However this annealing also leads to serious NP aggregation/sintering. Recently, we reported that, by coating the fcc-FePt NPs with a layer of MgO, high temperature annealing could convert the fcc-FePt/MgO to the fct-FePt/MgO without FePt aggregation.[6] The MgO coating was removed by a dilute acid wash, and ferromagnetic fct-FePt NPs could be stabilized by oleic acid and 1-hexadecanethiol and dispersed in hexane. Our further experiments indicated that once deposited on carbon supports, the FePt/MgO NPs could be transformed into FePt NPs without the presence of any surfactant, giving "clean" fcc-FePt or fct-FePt NPs that were ideal for catalytic studies. We found the fct-FePt NPs were more stable than fcc-FePt NPs and served as an active catalyst for ORR in 0.5 M H_2SO_4 solution.

The 8 nm fcc-$Fe_{48}Pt_{52}$/MgO NPs were synthesized as reported.[6] The fcc-FePt/MgO was converted to the fct-FePt/MgO at 750 °C for 6 h under 95% Ar + 5% H_2. Figure 1C shows the representative TEM image of the fct-FePt/MgO NPs after the thermal annealing. Compared with those before the annealing (Figure S1), FePt NPs in two samples show no morphology change. The structures and magnetic properties of these fcc-FePt/MgO and fct-FePt/MgO NPs were characterized by X-ray diffraction (XRD) (Figure S2) and vibrating sample magnetometry (VSM) (Figure S3), indicating the fct-FePt NPs are ferromagnetic while the fcc-FePt NPs are weakly superparamagnetic.[6]

The FePt/MgO NPs were deposited on the Ketjen carbon support (800 m^2/g) (FePt/C = 1/1 by weight) via a 1 h sonication[7] and immersed into the 0.5 M H_2SO_4 solution from 1 to 6 h. MgO was removed and the Fe, Pt composition after MgO removal was remeasured by energy dispersive X-ray spectroscopy (EDS) (Figure 1D). It can be seen that, within 1 h of immersion in the acid, the fcc-FePt NPs have a heavy Fe loss (36.5%) while the fct-FePt NPs show only a small Fe change (3.3%).

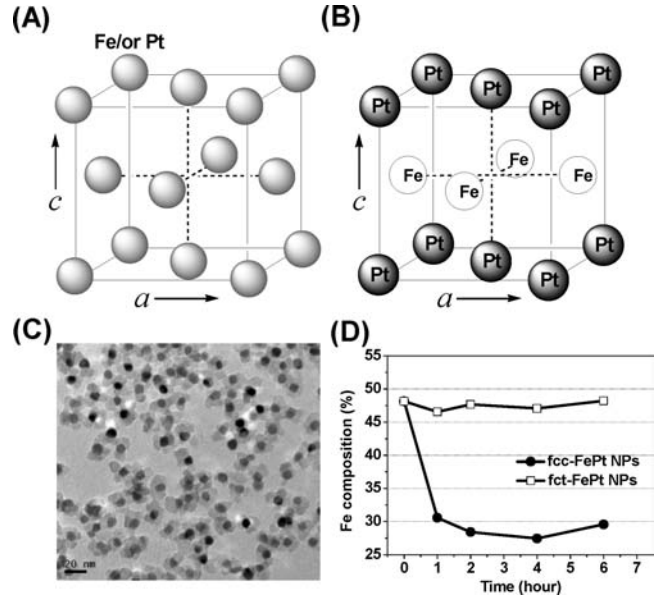

Figure 1. Schematic illustration of (A) chemically disordered fcc-FePt and (B) chemically ordered fct-FePt. (C) TEM image of the 8 nm fct-FePt/MgO NPs annealed at 750 °C for 6 h under Ar + 5% H_2. (D) Time-dependent composition changes of fcc- and fct-FePt NPs in 0.5 M H_2SO_4 solutions.

The fcc-FePt/C and fct-FePt/C catalysts (0.04 mg of each) along with the commercial 3.2 nm Pt/C NP catalyst (TEC10E50E from Tanaka Noble Metal Ltd.) (Figure S4) were deposited on the glassy carbon rotation disk electrode (RDE) and were evaluated for their catalytic ORR in 0.5 M H_2SO_4.[7] Cyclic voltammetry (CV) was scanned from −0.3 to 1.2 V at 50 mV/s to obtain the active surface area. All the CVs showed similar features to those of a typical polycrystalline Pt electrode (Figure S5).[8] The calculated surface areas in 0.5 M H_2SO_4 were 22.8 cm^2 for the commercial Pt/C, 6.70 cm^2 for the fcc-FePt/C, and 5.85 cm^2 for the fct-FePt/C. The area of the commercial Pt/C is larger than that of the fcc- and fct-FePt/C catalyst due to its smaller NP size and higher surface Pt concentration.[9] The ORR catalysis was studied in an oxygen saturated 0.5 M H_2SO_4 at room temperature in the potential range from 0.0 to 1.0 V. Figure 2A shows the $I-V$ curves related to the ORR process for three NP/C catalysts. We can see that both Pt/C and fcc-FePt/C have similar ORR onset potentials but the fct-FePt/C reduces this potential by nearly 100 mV. At the half-wave potential (0.53 V), the ORR current densities generated by the fct-FePt/C and the fcc-FePt/C are 3.5 and 2 times the value by the commercial Pt/C. This

[†] Current address: Department of Materials Science, California Institute of Technology, Pasadena, California 91125.

10.1021/ja1009629

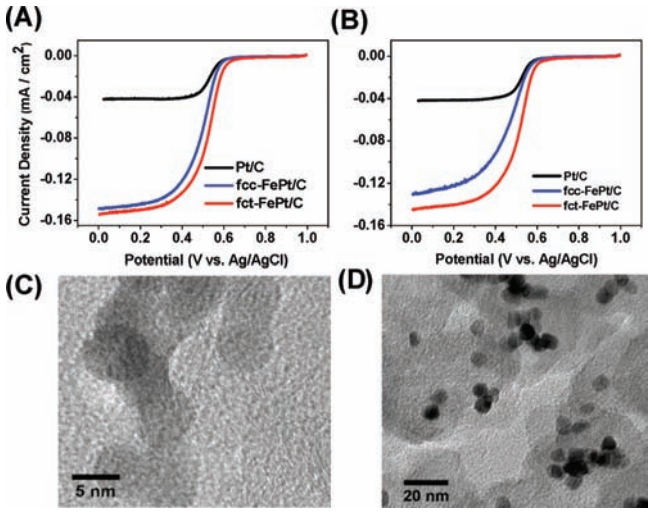

Figure 2. (A,B) ORR current densities from the commercial Pt/C, fcc-FePt/C, and fct-FePt/C catalysts in oxygen saturated 0.5 M H_2SO_4 before (A) and after (B) stability tests. The curves were measured with the RDE rotation speed of 1600 rpm and scan rate of 5 mV/s. (C,D) Typical TEM images of (C) fcc-FePt/C and (D) fct-FePt/C catalysts after stability tests.

ORR enhancement of the FePt catalyst is attributed to the Pt alloy with Fe, which changes both the geometric and electronic structures of Pt.[2] The fcc-FePt NPs have a lesser activity increase than the fct-FePt due to their heavy Fe loss in the 0.5 M H_2SO_4 solution.

The stability of the Pt/C, fcc-FePt/C, and fct-FePt/C catalysts for ORR was tested in the oxygen saturated 0.5 M H_2SO_4 at a scan rate of 50 mV/s for 1000 potential cycles. After these cycles, the $I-V$ curves were remeasured and were given in Figure 2B. The current densities at the half-wave potential were decreased by 20% for the commercial Pt/C, 27% for the fcc-FePt/C, and 14% for the fct-FePt/C catalysts. Figure 2C and D show the representative TEM images of the fcc-FePt/C and fct-FePt/C NPs after 1000 potential cycles. It can be seen that the majority of fct-FePt/C NPs stay well-dispersed on the carbon support, but the fcc-FePt NPs show some serious aggregation/sintering. EDS analyses on the FePt catalysts after the stability test revealed that the Fe content in the fcc-FePt/C dropped dramatically to Fe/Pt = 11:89, even more than the acid-etching test result shown in Figure 1D. In contrast, the fct-FePt NP catalyst showed only a slight change in the composition (Fe/Pt = 42:58) (Figure S6).

The enhanced ORR activity and durability of the fct-FePt vs fcc-FePt must be due to their well-ordered intermetallic structure seen in the fct-FePt NPs: (1) in the fct-FePt NPs, the Fe and Pt composition is much better preserved than that in the fcc-FePt in the acid solution and Pt stays active by the Fe alloy effect; (2) the intermetallic structure present in the fct-FePt offers some ideal catalytic facets around each NP with Pt sitting on the top and Fe lying under the Pt layer, a structural feature that is essential for catalytic enhancement;[1−3] (3) previous modeling studies on the fct-FePt structure show that, within the structure, Fe and Pt are strongly interactive via their spin−orbit coupling and the hybridization between Fe 3d and Pt 5d states makes the fct-FePt chemically much more stable.[10]

From the TEM image analysis, we can see that the fct-FePt NPs have slight morphology changes after the stability test. This could be the reason why the fct-FePt NPs show the small ORR activity drop (14%). Such a change is likely the result of the incomplete fcc to fct transition within the FePt structure during the annealing. The incomplete structure transition is evidenced from the magnetic hysteresis behavior of the FePt NPs. Without MgO coating, the fcc-FePt NPs are better converted to the fct-FePt with large coercivity (Figure S3), but the annealed NPs are seriously aggregated/sintered. Once the fcc-FePt NPs are embedded in the MgO matrix, the Fe, Pt mobility is limited during the annealing and complete structure transition to fct-FePt is difficult to achieve.[6] This can be seen in the magnetic hysteresis behavior of the fct-FePt/MgO NPs in which a kink appears near 0 G field due to the presence of the superparamagnetic fcc-FePt (Figure S3).

The ORR activity and durability of the fcc-FePt and fct-FePt NPs were also tested in 0.1 M $HClO_4$ solution. The results showed that they were active for ORR but had comparable stability. After 1000 potential cycles in oxygen saturated 0.1 M $HClO_4$, they showed similar aggregation behavior (Figure S7). It seems that, under the current test conditions, the FePt NPs are not suitable for ORR catalysis in $HClO_4$.

In summary, this work explores a unique feature of FePt/MgO NPs and studies their catalysis for ORR in 0.5 M H_2SO_4 solution. Due to the MgO coating, the FePt/MgO can be annealed at high temperatures and fcc-FePt is converted to fct-FePt. More significantly, the MgO coating can be removed by a dilute H_2SO_4 wash, leaving a "clean" FePt surface that is suitable for catalytic studies. The fct-FePt NPs are more active and durable than the fcc-FePt NPs for ORR in 0.5 M H_2SO_4 due to its stable intermetallic Fe, Pt arrangement. The results show that the activity and durability of the Pt-based alloy NP catalyst are dependent not only on its composition but also on its structure. The study further indicates that the fully ordered fct-FePt or other MPt could serve as a practical Pt-based catalyst for fuel cell applications.

Acknowledgment. The work was supported by a DOE/EERE program, by a Brown Seed Fund, and in part by the DOE/DE-SCOOO1556 and a GAANN fellowship (Y.L.)

Supporting Information Available: Synthesis of FePt nanoparticles and characterizations. This material is available free of charge via the Internet at http://pubs.acs.org.

References

(1) (a) Stamenkovic, V. R.; Mun, B. S.; Arenz, M.; Mayrhofer, K. J. J.; Lucas, C. A.; Wang, G.; Ross, P. N.; Markovic, N. M. *Nat. Mater.* **2007**, *6*, 241–247. (b) Stamenkovic, V. R.; Schmidt, T. J.; Ross, P. N.; Markovic, N. M. *J. Electroanal. Chem.* **2003**, *554*, 191–199. (c) Paulus, U. A.; Wokaun, A.; Scherer, G. G.; Schmidt, T. J.; Stamenkovic, V.; Radmilovic, V.; Markovic, N. M.; Ross, P. N. *J. Phys. Chem. B* **2002**, *106*, 4181–4191.

(2) (a) Greeley, J.; Stephens, I. E. L.; Bondarenko, A. S.; Johansson, T. P.; Hansen, H. A.; Jaramillo, T. F.; Rossmeisl, J.; Chorkendorff, I.; Nørskov, J. K. *Nat. Chem.* **2009**, *1*, 552–556. (b) Stamenkovic, V. R.; Fowler, B.; Mun, B. S.; Wang, G.; Ross, P. N.; Lucas, C. A.; Markovic, N. M. *Science* **2007**, *315*, 493–497.

(3) (a) Stamenkovic, V.; Schmidt, T. J.; Ross, P. N.; Markovic, N. M. *J. Phys. Chem. B* **2002**, *106*, 11970–11979. (b) Toda, T.; Igarashi, H.; Uchida, H.; Watanabe, M. *J. Electrochem. Soc.* **1999**, *146*, 3750–3756. (c) Mukerjee, S.; Srinivasan, S.; Soriaga, M. P. *J. Electrochem. Soc.* **1995**, *142*, 1409–1422.

(4) (a) Sun, S.; Murray, C. B.; Weller, D.; Folks, L.; Moser, A. *Science* **2000**, *287*, 1989–1992. (b) Chen, M.; Liu, J. P.; Sun, S. *J. Am. Chem. Soc.* **2004**, *126*, 8394–8395.

(5) (a) Sun, S. *Adv. Mater.* **2006**, *18*, 393–403. (b) Brown, G.; Kraczek, B.; Janotti, A.; Schulthess, T. C.; Stocks, G. M.; Johnson, D. D. *Phys. Rev. B* **2003**, *68*, 052405. (c) Gutfleisch, O.; Lyubina, J.; Muller, K.-H.; Schultz, L. *Adv. Eng. Mater.* **2005**, *7*, 208–212.

(6) (a) Kim, J.; Rong, C.; Liu, J. P.; Sun, S. *Adv. Mater.* **2009**, *21*, 906–909. (b) Kim, J.; Rong, C.; Lee, Y.; Liu, J. P.; Sun, S. *Chem. Mater.* **2008**, *20*, 7242–7245.

(7) See the Supporting Information

(8) (a) Wang, J. X.; Markovic, N. M.; Adzic, R. R. *J. Phys. Chem. B* **2004**, *108*, 4127–4133. (b) Lim, B.; Jiang, M.; Camargo, P. H. C.; Cho, E. H.; Tao, J.; Lu, X.; Zhu, Y.; Xia, Y. *Science* **2009**, *324*, 1302–1305. (c) Zhang, J.; Sasaki, K.; Sutter, E.; Adzic, R. R. *Science* **2007**, *315*, 220–222.

(9) Chen, W.; Kim, J.; Sun, S.; Chen, S. *J. Phys. Chem. C* **2008**, *112*, 3891–3898.

(10) (a) Staunton, J. B.; Ostanin, S.; Razee, S. S. A.; Gyorffy, B. L.; Szunyogh, L.; Ginatempo, B.; Bruno, E. *Phys. Rev. Lett.* **2004**, *93*, 257204. (b) Burkert, T.; Eriksson, O.; Simak, S. I.; Ruban, A. V.; Sanyal, B.; Nordström, L.; Wills, J. M. *Phys. Rev. B* **2005**, *71*, 134411.

JA1009629